Environmental Microbiome

RESEARCH Open Access

Crop genotype modulates root rot resistance-associated microbial community composition and abundance of key taxa

Valentin Gfeller[1*], Michael Schneider[1], Natacha Bodenhausen[2], Matthew W. Horton[1], Lukas Wille[1], Klaus H. Oldach[3], Bruno Studer[4], Martin Hartmann[5], Monika M. Messmer[1] and Pierre Hohmann[1,6*]

Abstract

Background Plants are constantly challenged by pathogens, which can cause substantial yield losses. The aggressiveness of and damage by pathogens depends on the host-associated microbiome, which might be shaped by plant genetics to improve resistance. How different crop genotypes modulate their microbiota when challenged by a complex of pathogens is largely unknown. Here, we investigate if and how pea (*Pisum sativum L.*) genotypes shape their root microbiota upon challenge by soil-borne pathogens and how this relates to a genotype's resistance. Building on the phenotyping efforts of 252 pea genotypes grown in naturally infested soil, we characterized root fungi and bacteria by ITS region and 16 S rRNA gene amplicon sequencing, respectively.

Results Pea genotype markedly affected both fungal and bacterial community composition, and these genotype-specific microbiota were associated with root rot resistance. For example, genotype resistance was correlated ($R^2 = 19\%$) with root fungal community composition. Further, several key microbes, showing a high relative abundance, heritability, connectedness with other microbes, and correlation with plant resistance, were identified.

Conclusions Our findings highlight the importance of crop genotype-specific root microbiota under root rot stress and the potential of the plant to shape its associated microbiota as a second line of defense.

Keywords *Pisum sativum*, Plant-microbe interaction, Resistance breeding, Pea root rot, Grain legumes, Microbiota heritability

*Correspondence:
Valentin Gfeller
valentin.gfeller@fibl.org
Pierre Hohmann
pierre.hohmann@ub.edu
[1]Plant Breeding, Department of Crop Sciences, Research Institute of Organic Agriculture (FiBL), Frick, Switzerland
[2]Nutrient Management and Symbiosis, Department of Soil Sciences, Research Institute of Organic Agriculture (FiBL), Frick, Switzerland
[3]Pre-Breeding Barley, Oats and Pulses, KWS LOCHOW GMBH, Bergen, Germany
[4]Molecular Plant Breeding, Department of Environmental Systems Science, ETH Zurich, Zurich, Switzerland
[5]Sustainable Agroecosystems, Department of Environmental Systems Science, ETH Zurich, Zurich, Switzerland
[6]Department of Biology, Healthcare and the Environment, Faculty of Pharmacy and Food Sciences, Universitat De Barcelona, Barcelona 08028, Spain

Introduction

Plant-associated microbiomes can promote plant health in many ways [1, 2]. A balanced microbiota, including bacteria, is essential for plants to protect themselves against pathogens and survive [3]. To benefit from such beneficial microbiome-dependent services, plants shape the microbiota in their surrounding environment [4, 5]. This provides a promising tool to engineer a crop's microbiome through host genetics [6]. Genotype-specific plant microbiome interactions affect not only the focal plant but also the growth and defense of succeeding plants in that soil [7], which is particularly interesting in the context of crop rotation. For example, a mechanism to cope with the growth-suppressive effects of precrop-specific microbiota in the soil is the exudation of root secondary metabolites [8]. Therefore, to enhance the resistance of grain legumes against crop rotation-specific soil-borne pathogens, the modulation of plant-microbiota interaction through breeding might also offer a promising approach [9].

Crop pathogens pose a major threat to global food security and their negative effects are expected to be further amplified by climate change [10, 11]. Pathogen suppression by plant-associated microbiota poses a promising, new approach to manage crop diseases sustainably [12, 13]. It is known that the composition of the resident microbiota determines, together with the plant's innate immune system, whether a certain microbe acts as a pathogen, commensal, or even beneficial [14–16]. It has been shown that plants can enrich specific taxa from the surrounding soil microbiome around their roots, thereby reducing pathogen aggressiveness and promoting plant growth [17, 18]. Banana plants, for example, can enrich beneficial fungi through specific plant exudates that confer resistance against the pathogen Foc TR4 [18]. Such microbe-mediated disease resistance can be triggered by direct antagonisms like antimicrobial molecules and niche competition [19–22], or indirectly through the activation of the host immune system [23, 24]. Further, the endophytic root microbiota can confer induced resistance upon pathogen attack [25]. While it is established that the microbiota can mediate pathogen suppression of plants, the frequency of this phenomenon across different plants and the relative contribution of this mechanism in comparison to direct plant defense remains to be elucidated [13, 26].

Pea (*Pisum sativum*, L.) belongs to the most frequently cultivated legumes worldwide [27]. Their symbiosis with nitrogen-fixing rhizobia can increase soil fertility, providing a benefit for themselves and subsequently cultivated crops and the peas also serve as high-quality, protein-rich food and feed [27, 28]. Along with other legumes, pea production is highly constrained by soil-borne pathogens, which build up upon repeated legume cropping and cause severe wilt and root rot, also known as soil fatigue, which can lead to considerable yield losses [29, 30]. Several pathogenic fungi and oomycetes can be part of the root rot complex, with the most reported causal agents being *Aphanomyces euteiches*, *Didymella pinodes*, *Didymella pinodella*, *Fusarium avenaceum*, *Fusarium oxysporum*, *Fusarium redolens*, *Fusarium solani*, *Pythium* sp., and *Rhizoctonia solani* [29–34]. First evidence suggests that the synergistic effect of these pathogens increases their aggressiveness, and thus, makes resistance breeding even more challenging [35–37]. Plant breeding for microbiota-dependent disease resistance could assist in overcoming this challenge [6]. Screening of a pea diversity panel grown in naturally infested soil showed considerable variation in disease resistance across different pea lines [38]. An in-depth analysis of eight genotypes in four different soils revealed predefined fitness-associated microbial markers as predictors for root rot resistance, including arbuscular mycorrhizal fungi [39]. While microbiota communities of peas grown in healthy and infested soils have been compared and shown to differ [40, 41], it is largely unknown how different pea lines interact with their microbiota under root rot.

In this study, we investigate if and how pea lines with diverse resistance levels against root rot interact with their microbiota. Our key hypothesis was that pea plants modulate their root microbiota under root rot stress in a genotype-specific manner and that this relates to a genotype's resistance - two prerequisites for microbiome-assisted resistance breeding. We examined the fungal and bacterial microbiota of a diverse panel of 252 pea genotypes, consisting of gene bank accessions, breeding lines, and registered cultivars grown in a climate chamber under root rot stress. Associations of pea resistance with alpha diversity, microbial community composition, and individual taxa were investigated. Furthermore, we determined the proportion of variation in OTU abundance and microbiota diversity explained by host genotype (hereafter heritability or H^2) and performed network analyses. We found associations between microbial diversity measures and resistance levels, as well as taxa associated with resistance, which were also shown to be heritable and connected within the root microbiota. This illustrates the potential of microbiota-mediated resistance breeding against legume root rots.

Materials and methods

Plant material

We capitalized on root samples collected from a previous study [38]. A diverse set of 261 pea genotypes was grown under root rot stress. To eliminate confounding effects due to seed age and origin, the pea seeds were multiplied in a common environment (Sativa Rheinau AG, Switzerland) prior to the experiment. In this study,

we investigated the root microbiota of a subset of 252 pea genotypes originating from three seed sources: 173 gene bank accessions of the USDA pea core collection, 33 registered European cultivars, and 46 advanced breeding lines from a Swiss plant breeder (Getreidezüchtung Peter Kunz). Two European cultivars were selected as reference lines based on their known partial resistance (EFB.33: "C1") and susceptibility (Respect: "C2") to root rot.

Characterization of root rot resistance

To study the root microbiota of the pea panel under root rot stress, a resistance assay was performed under controlled conditions as described by Wille et al. (2020). A pH neutral loam soil naturally infested by pea root rot pathogens was collected on a field under certified organic production in Kirchlindach, Switzerland (47°00′14.5″N 7°24′37.7″E). To determine the growth potential of the genotypes in pathogen-free soil and evaluate the performance-reduction through soil infestation, a subset of the collected soil was X-Ray sterilized (30–100 kGy for 4 h, Synergy Health Däniken AG, Switzerland). This sterilization method has also proven effective in other studies to determine the effect of soil microbiota on plant vigor [7, 39]. Infested and sterilized soils were mixed with autoclaved quartz sand in a 2:1 (v: v) ratio and filled into plastic pots (200 ml) to improve soil structure. Four seeds per pot were surface sterilized with ethanol and bleach and soaked in water before sowing. Each pea genotype was grown in four pots (replicates) in either infested or sterilized soil in a randomized block design. Plants were grown in a walk-in climate chamber at 20 °C, 85% relative humidity, and 16 h of light per day. The soil was kept moist by flooding the pots 4 cm high with water every 72 h for 30 min, as determined by prior optimization trials. The total number of emerged seedlings was recorded 14 days after sowing. Plants were harvested and phenotyped at 21 days. Shoot dry biomass was determined, and relative shoot dry weight was calculated by dividing the mean weight per plant in the infested soil by the mean weight in the sterilized soil (SDW_{Rel}). In addition, relative total shoot biomass per pot ($tSDW_{Rel}$) was calculated as described before but considering the biomass of all germinated plants within one pot. To evaluate belowground disease levels, plants were removed from the pots and cleaned with tap water. The root rot index (RRI: 1 = no symptoms, 3 = light brown discoloration and moderate disintegration of the root system, 6 = completely disintegrated root system) was determined as previously described [38], and median values per pot were used for analysis. For microbiota analysis, the previously phenotyped roots of the plants grown in infested soils were pooled per pot and sampled as described in Lundberg et al. (2012). Briefly, soil was removed by shaking the roots with sterile gloves, followed by a washing step in 25 ml of sterile water in a 50 ml tube by vortexing vigorously. Clean roots were stored at -20 °C until lyophilization with an Alpha 1–4 LSC freeze dryer (Christ, Osterode am Harz, Germany) before they were milled to fine powder in a steel jar with one 20 mm steel ball utilizing a ball mill (Retsch, Haan, Germany) at 25 Hz for 20 s.

Microbiota profiling

DNA extraction and amplicon sequencing

For all plants grown in infested soils, DNA extraction was carried out with 15 mg of dry root powder using the Mag-Bind Plant DNA DS 96 Kit (Omega Bio-Tek, Norcross, United States) following the manufacturer's instructions. Integrity and concentration of the extracted DNA were checked using gel electrophoresis and Qubit 4 (Thermo Fischer Scientific, Waltham, Massachusetts, US) before dilution to 10 ng/ul and shipped along with negative controls to the Genome Quebec Innovation Center (Montreal, Canada) for library preparation and sequencing.

At the Genome Quebec Innovation Center, libraries were prepared and sequenced for the entire internal transcribed spacer (ITS) region (fungi, see below) and the V3 and V4 hypervariable regions of the 16 S rRNA gene (bacteria, see below), including positive and negative amplification controls. Controls were visualized together with samples by gel electrophoresis to confirm that the amplification was successful and rule out contamination. They performed as expected and were not sequenced. For DNA extraction, shipment, library preparation, and sequencing, samples were distributed randomly across plates and libraries.

For the fungal libraries, the amplicon libraries were prepared in a 2-step PCR process following the Pacific Biosciences Barcoded Universal Primers for Multiplexing Amplicons Template Preparation and Sequencing protocol to sequence the entire ITS region. In the first PCR step, the target region was amplified with the ITS1F [42] and ITS4 [43] primers coupled to CS1 and CS2 linker using the HotStarTaq DNA Polymerase (Qiagen, Hilden, Germany). The PCR reaction contained 1x PCR buffer with 1.5 mM $MgCl_2$, 5% DMSO (Roche, Basel, Switzerland), 0.2 mM dNTP mix (NEB, Ipswich, Massachusetts, US), 0.02 U/ul HotStarTaq DNA Polymerase (Qiagen), 0.6 µm of each primer and 10 ng DNA in a reaction volume of 25 ul. The PCR conditions included an initial step at 96 °C for 15 min, 33 cycles of 96 °C for 30 s, 52 °C for 30 s and 72 °C for 60 s, ending with a final extension at 72 °C for 10 min. For the second PCR reaction (multiplexing PCR), barcoded primers were utilized and bound to the amplicons of the first PCR via the linker sequences CS1 and CS2 using the FastStart High Fidelity PCR System (Roche). The PCR reaction contained 1x PCR buffer without $MgCl_2$, 1.8 mM $MgCl_2$ (Roche), 5% DMSO

(Roche), 0.2 mM dNTP mix (NEB), 0.025 U/ul FastStart High Fidelity DNA Polymerase (Roche), 0.1 µm of each barcoding primer and 1 ul of DNA from PCR 1 previously diluted 1:50 in a reaction volume of 20 ul. The PCR conditions included an initial step at 95 °C for 10 min, 15 cycles of 95 °C for 15 s, 60 °C for 30 s and 72 °C for 60 s, ending with a final extension at 72 °C for 3 min. For the library construction no DNA shearing was performed since the samples were amplicons, and 1,000 ng of purified amplicons were used. The DNA Damage repair, End repair, and SMRT bell ligation steps were performed as described in the template preparation protocol with the SMRTbell Template Prep Kit 2.0 reagents (Pacific Biosciences, Menlo Park, CA, US). The sequencing primer was annealed with sequencing primer v4 at a final concentration of 1 nM, and the Sequel II 2.1 polymerase was bound at 0.5 nM. The libraries went through an AMPure bead cleanup (following the SMRTlink calculator procedure) before being sequenced in four runs on a PacBio Sequel II instrument at a loading concentration between 120 pM and 200 pM using the diffusion loading protocol, Sequel II Sequencing kit 2.0, SMRT Cell 8 M and 10 h movies with no pre-extension.

For the bacterial libraries, the amplicon libraries were prepared in a 2-step PCR process to the V3 and V4 hypervariable regions of the 16 S rRNA gene. In the first PCR step, the target region was amplified with the V3F [44] and 799R [45] primers coupled to CS1 and CS2 linker using the Q5 High-Fidelity DNA Polymerase (NEB). The PCR reaction contained 1x reaction buffer, 5% DMSO (Roche), 0.2 mM dNTP mix (NEB), 0.02 U/ul Q5 High-Fidelity DNA Polymerase (NEB), 0.6 µm of each primer and 10 ng DNA in a reaction volume of 25 ul. The PCR conditions included an initial step at 98 °C for 0.5 min, 26 cycles of 98 °C for 10 s, 58 °C for 15 s and 72 °C for 30 s, ending with a final extension at 72 °C for 2 min. For the second PCR reaction (multiplexing PCR), barcoded primers were utilized and bound to the amplicons of the first PCR via the linker sequences CS1 and CS2 using the FastStart High Fidelity PCR System (Roche). The PCR reaction contained 1x PCR buffer without $MgCl_2$, 1.8 mM $MgCl_2$ (Roche, Basel, Switzerland), 5% DMSO (Roche), 0.2 mM dNTP mix (NEB), 0.025 U/ul FastStart High Fidelity DNA Polymerase (Roche), 0.1 µm of each barcoding primer and 1 ul of DNA from PCR 1 previously diluted 1:100 in a reaction volume of 20 ul. The PCR conditions included an initial step at 95 °C for 10 min, 15 cycles of 95 °C for 15 s, 60 °C for 30 s and 72 °C for 60 s, ending with a final extension at 72 °C for 3 min. The barcoded libraries were first normalized to 2 nM, then pooled and denatured in 0.05 N NaOH. The pool was diluted to 9 pM using HT1 buffer and was loaded on a MiSeq and sequenced in three runs for 2 × 300 cycles according to the manufacturer's instructions. A phiX library was used as a control and mixed with libraries at 12% level. The MiSeq Control Software (MCS) version was 2.5.0.5, and RTA version was 1.18.54. The program bcl2fastq v1.8.4 was then used to demultiplex samples and generate fastq reads. The demultiplexed sequences have been deposited in the European Nucleotide Archive (ENA) under the accession code PRJEB83630.

Sequence data processing

For the fungal PacBio sequences, the bioinformatic analysis was performed at the Genetic Diversity Centre at ETH Zurich (Switzerland). In short, raw high-quality CCS reads were quality-filtered (min length: 400 bp, max Ns: 0, max low-complexity: 30%) using UPARSE [46], and error-corrected to obtain zero radius operational taxonomic units (zOTUs) using UNOISE [47]. zOTUs are conceptually equivalent to ASVs generated through *DADA2* [48]. The zOTUs were further clustered into fungal OTUs (fOTUs) of 97% nucleotide similarity with UPARSE [46], to avoid splitting one microorganism into several zOTUs (or ASVs) due to intragenomic heterogeneity known for the ITS region and the 16 S rRNA gene [49–52]. For each OTU, the most abundant sequence (zOTU) was selected as representative. Taxonomic associations were predicted using the SINTAX classifier [53] with the UNITE (v8.3, released May 10, 2021; [54]) ITS reference database. For bacterial Illumina sequences, bioinformatics was performed in QIIME2 (version qiime2-2021.4) [55] as previously described [56]. Briefly, after importing the demultiplexed sequences, primers were removed using *cutadapt* (v1.16 implemented in QIIME2). Utilizing the *DADA2* pipeline (v1.18 [48]), the raw reads were quality filtered (maxEE: 2; maxN: 0), truncated at positions 219 (forward) and 221 (reverse), based on visual inspection of quality plots, and shorter and low-quality reads (truncQ = 2) were discarded. Trimmed reads were denoised, and exact amplicon sequences (ASVs) were inferred. ASVs were then clustered into bacterial OTUs (bOTUs) of 97% nucleotide similarity using *vsearch* (v2.7.0 [57]). For each OTU, the most abundant sequence (ASV) was selected as representative. Taxonomy was assigned using the SILVA database (v138, released December 16, 2019; [58]) and the naive Bayesian classifier method implemented in QIIME2 [59].

Statistical analysis

All statistical analyses were conducted using the open-source software R v.4.3.0 [60]. Data wrangling and visualization were facilitated with the *tidyverse* package collection [61], as well as *ggbeeswarm* and *cowplot* for visualization [62, 63]. The *phyloseq* R package facilitated microbiota analysis [64]. After importing bacterial and fungal count and taxonomy tables, unwanted samples or OTUs were filtered out before microbiota analysis.

First, two fOTUs belonging to host DNA and the Kingdom Rhizaria according to the UNITE database and 61 bOTUs unassigned at the Kingdom level or assigned to eukaryotes, mitochondria, or chloroplasts according to the SILVA database were removed. To remove low-quality samples, five samples with less than 1,000 fungal sequences and one sample with less than 11,000 bacterial sequences were excluded. Further, 54 previously identified pea lines [38] with heterogeneous seed or flower appearance were also excluded because they were assumed to be genetically heterozygous. Lastly, low-abundance OTUs were removed, if not present with at least four sequences in at least four samples. Data filtering, transformation, and analysis are summarized in Figure S1.

Alpha diversity was analyzed for fungi and bacteria separately by first rarefying the data to 1,000 fungal sequences and 11,000 bacterial sequences using the *vegan* package [65] and then calculating the OTU richness and Shannon diversity index in each sample based on the mean of 1,000 iterations. To test the effects of pea genotype and seed source (gene bank accessions, breeding material, registered cultivars) on alpha diversity, an Analysis of Variance (ANOVA) was performed. Statistical assumptions, i.e., normal distribution and homoscedasticity of error variance, were visually checked. Differences among Estimated Marginal Means (EMMs) of seed sources were tested using the *emmeans* package [66], taking the Tukey method for *P* value adjustment for multiple testing and using compact letter display using the *multcomp* package for visualization [67]. We further checked for correlations of alpha diversity with resistance-associated traits: Spearman correlations were calculated for ordinal data and Pearson correlations were performed for continuous variables.

We further examined how the microbial community composition (beta diversity) of fungal and bacterial communities relates to pea genotype, seed source, and resistance traits. Effects were visualized by Principal Coordinates Analysis (PCoA) ordination using Bray-Curtis dissimilarity matrices and tested by Permutational Multivariate Analysis of Variance (PERMANOVA) using the *adonis2* function from the *vegan* package [65]. Multivariate homogeneity of dispersion (variance) between the seed sources was tested using the *betadisper* function from the *vegan* package [65]. The combination of PERMANOVA and *betadisper* allows us to distinguish between location and dispersion effects in beta diversity analysis [68]. We also tested whether the association between the resistance trait and the beta diversity depends on the seed source by including the interaction term of the two variables in the fitted model (model: beta diversity ~ resistance trait * seed source). To test how the average phenotype of each genotype influences the community compositions, PCoA and PERMANVOA were also performed on mean values per genotype. Another PERMANVOA was performed to estimate the variation explained (R^2) by the experimental replicates (blocks).

To evaluate the proportion of variation in root microbiota diversity indices and of the relative abundance of individual OTUs that is explained by the host genotype, we calculated the broad-sense heritability (H^2). The count tables were first normalized by centered log-ratio (clr) transformation with the *aldex.clr* function implemented in the R package *ALDEx2* [69], as relative abundance matrices can lead to misinterpretation of OTU heritability [70]. H^2 was calculated as the proportion of variance explained by the random intercept effect (here, pea genotype) as described before [71]. To accomplish this, we fitted a linear mixed-effects model (y ~ 1|'pea genotype') using the *lme* function from the *lme4* R package [72] for alpha diversity (OTU richness and Shannon diversity index), beta diversity (PCo axis 1) and clr-transformed abundance of OTUs. To account for within-genotype variation, the replicate identity was included in the model as a fixed factor. Bootstrap confidence intervals (95%) were computed using the *bootMer* function from the *lme4* R package [72] using 999 bootstraps. Differences between the median heritability of fungal and bacterial OTUs were tested by a two-sided Wilcoxon rank sum test. To assess whether there are more fungal OTUs within the 58 most heritable OTUs ($H^2 > 20\%$), we performed a binomial test using the *binom.test* function.

To identify OTUs that are associated with root rot resistance, we performed differential abundance analysis for individual OTUs. The R package *ALDEx2* [69] was chosen for the analysis as it has been shown to produce consistent results across studies [73]. Count tables were clr-transformed with the *aldex.clr* function before a Spearman correlation was performed using the *aldex.corr* function. A specific OTU was considered associated with resistance when $P < 0.05$ after Benjamini-Hochberg correction for multiple testing [74]. To visualize the number of OTUs that associate with individual or multiple resistance traits, an UpSet plot showing all observed intersections was generated using the *scale_x_upset* from the *ggupset* package [75]. OTUs that significantly correlated with all resistance traits were further visualized in a heat map using the *plot_heatmap* from the *phyloseq* package [64].

To identify highly connected (hub) OTUs, we made use of network inference. Bacterial and fungal count tables were combined before running the 'SParse InversE Covariance Estimation for Ecological ASsociation Inference' (SPIEC-EASI) pipeline [76]. This pipeline has been demonstrated to perform robust cross-domain network analyses, exhibiting higher connectivity and increased

network stability compared to single-domain networks [71, 77]. SPIEC-EASI was executed using the neighborhood selection method to compute the network. Network analyses were facilitated by the R package *igraph* [78]. Betweenness centrality and degree were taken as measures for connectedness; the two measures are defined as the number of shortest paths going through a node (betweenness) and the number of its adjacent edges (degree). OTUs belonging to the top 10% of betweenness or the top 10% of degree were considered as hub OTUs.

To summarize the OTUs of most interest, we selected highly heritable (top 10%) hub OTUs that were also associated with root rot resistance (top 10% in correlations with at least one resistance-associated trait) and showed a relative abundance above 1%. These OTUs were further taxonomically investigated. Besides the above-mentioned taxonomic assignment, we further investigated the taxonomy by performing a standard nucleotide blast to the NCBI database using the representative OTU sequences. If more than one taxonomic entry showed the maximum percentage identity at the maximum query coverage, the next higher taxonomic level was indicated. The same procedure was performed for OTUs belonging to taxonomic groups that are expected to be involved in root rot and resistance to it [39].

We further investigated how best to model disease resistance using measures of OTU abundance and beta diversity. Seedling emergence and RRI were modeled through four models: (i) A stepwise regression on the 20 most abundant OTUs and the two first PCo axes (beta diversity) of both domains (bacteria and fungi), performed with the *stepAIC* function from the *MASS* package [79] using backward selection direction; (ii) A stepwise regression on these (40) OTUs only; (iii) A simple linear model with the PCo axis showing the highest correlation; (iv) A simple linear model with the OTU showing the highest correlation. The models were compared based on Akaike's information criterion (AIC), adjusted R^2 and the corresponding *P* value.

Results

Microbial diversity is affected by pea genotype under root rot stress

Amplicon sequencing provided 6,726 ± 4,294 (mean ± SD) fungal and 26,471 ± 6,781 bacterial sequences per sample, with variable coverage across sequencing runs calling for data normalization prior to downstream analysis (Figure S1, Figure S2). A first inspection of the most abundant taxa in our data revealed that the most abundant phyla were Ascomycota in the fungal Kingdom and Proteobacteria in the bacterial domain (Figure S3). We found a few genera that contributed to a large fraction of the microbiota. For Fungi, 19% of the reads were assigned to the genus *Dactylonectria* and 12% to *Fusarium*. For Bacteria, 49% of the reads were assigned to possibly nodule-inhabiting *Rhizobium* spp. (SILVA databank genus taxonomy: "Allorhizobium-Neorhizobium-Pararhizobium-Rhizobium"), 15% to *Flavobacterium* spp. and 9% to *Pseudomonas* spp.

To examine the variation within our data set, we first compared alpha diversity indices among pea genotypes and seed sources, where the seed source reflects different levels of breeding intensity. The plant genotype explained 16% and 25% of the variation in fungal and bacterial Shannon diversity, respectively, whereas the seed source explained only 1–2% of the variation (Fig. 1). Similar patterns were observed for OTU richness (Figure S4). The most consistent difference in alpha diversity among the seed sources was found between the gene bank material and the breeding material, where Shannon diversity and OTU richness were reduced in the genotypes originating from the gene bank.

Similar to alpha diversity, the plant genotype explained a large fraction of the microbial beta diversity (45–51%), whereas the influence of the seed source was relatively small (1–4%) (Fig. 2), as revealed by PERMANOVA. Visualization of the first two axes of a Principal Coordinates Analysis (PCoA) confirmed the spatial separation of the two reference genotypes (EFB.33 and Respect) and the absence of a strong seed source effect. For fungi, gene bank accessions also showed an enhanced multivariate dispersion compared to the other seed sources (Figure S5). For unbalanced designs where the larger group has a greater dispersion, as in this case, the test might be overly conservative [68].

Variation in microbial diversity is associated with root rot resistance

The analyzed pea genotypes have been shown to differ strongly in their resistance to root rot ([38] and Fig. 3). To evaluate the interplay between disease resistance and root microbial diversity, we tested for associations between alpha diversity indices and root rot phenotypes (emergence and RRI). For bacteria, an increase in Shannon diversity and OTU richness was associated with reduced seedling emergence and higher RRI, which was most pronounced for Shannon diversity and RRI ($R^2 = 9.4\%$, Figure S6, Figure S7). In contrast, less striking and inconsistent associations were found for fungi.

PERMANOVA and visualization of PCoA revealed a significant link between all resistance-associated traits and beta diversity in both domains (Fig. 3a, b). For fungi, traits with the strongest association were found to be emergence ($R^2 = 9.3\%$) and relative total shoot dry weight per pot ($tSDW_{Rel}$, $R^2 = 9.4\%$; Fig. 3a). In contrast, for bacterial communities, the strongest association was found for RRI ($R^2 = 8.6\%$, Fig. 3b). When calculated on mean values per genotype, the explained variation for

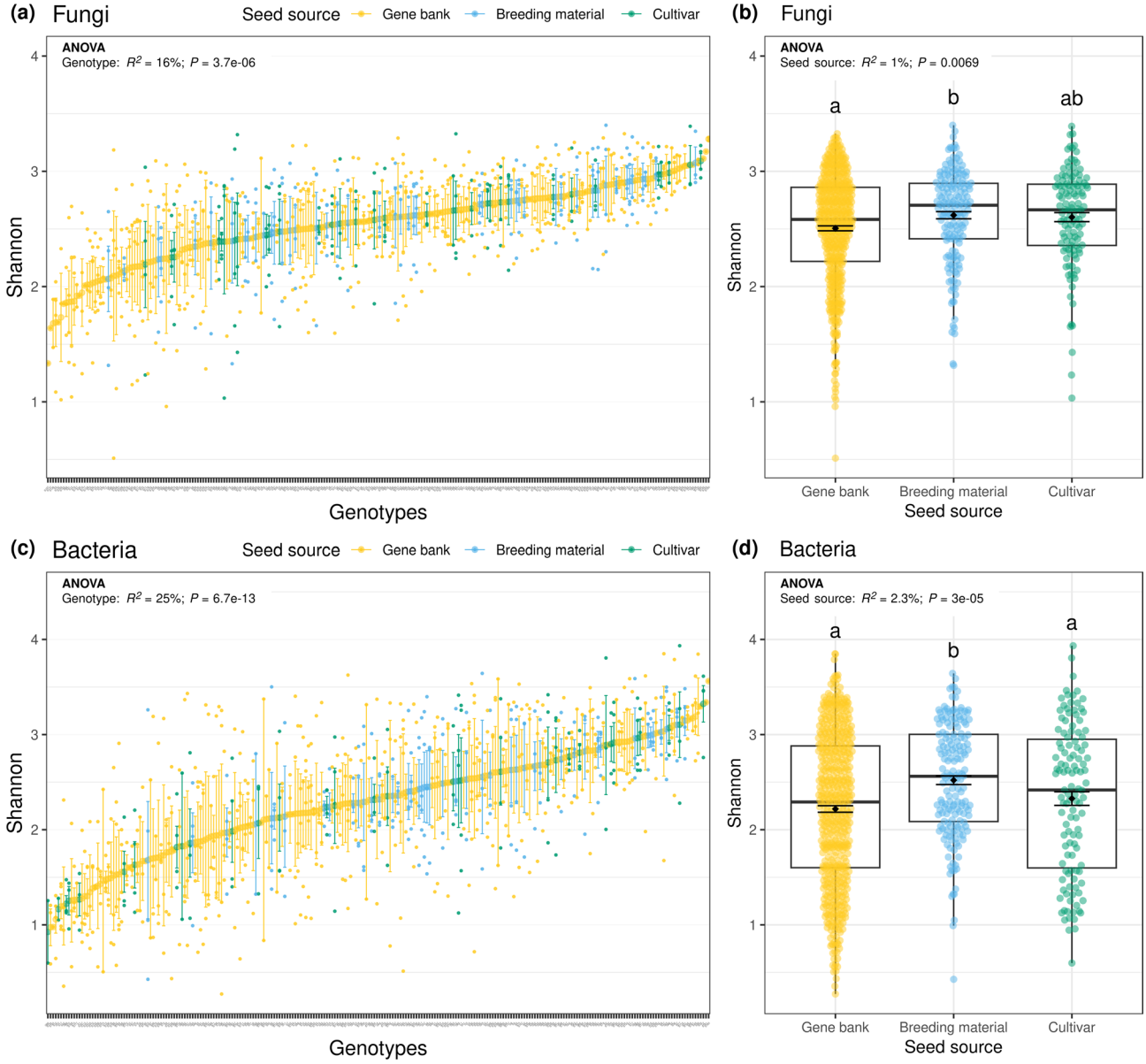

Fig. 1 Influence of plant genotype **(a**, **c)** and seed source **(b**, **d)** on root fungal **(a**, **b)** and bacterial **(c**, **d)** alpha diversity. All plots show individual datapoints, means ± SE, and the ANOVA results with the explained variance (adjusted R^2) and the corresponding *P* value. In **(b)** and **(d)** boxplots are also shown. Letters indicate significant differences among seed sources (analysis of variance followed by pairwise comparison of estimated marginal means, $P_{adj} < 0.05$)

microbial community composition increased approximately two-fold for fungi ($R^2_{emergence}$ = 19%, Fig. 3c) and bacteria (R^2_{RRI} = 14%, Figure S8), demonstrating that there was considerable within-genotype variation (replicate and stochastic effects) in our study system. Another PERMANOVA revealed that the experimental replicate only showed a minor but statistically significant effect on the community composition (fungi: $R^2_{replicate}$ = 0.97%; bacteria: $R^2_{replicate}$ = 1.9%). Interestingly, we found that the association between emergence and fungal community composition depended on the seed source, as shown by a statistically significant interaction term between the two variables in PERMANOVA ($R^2_{emergence\ x\ 'seed\ source'}$ = 2.2%, Fig. 3a, c). No such dependence on seed source was found for bacterial communities (Figure S8). To further disentangle the interdependency of resistance and seed source in fungal beta diversity, we performed an ANOVA followed by individual correlation analyses for each seed source between community composition (PCo axis 1) and emergence (Fig. 3d). Again, we observed that beta diversity is associated with seed source, emergence, and their interaction. Correlating community composition and emergence within each seed source separately, we found a statistically significant link for the gene bank

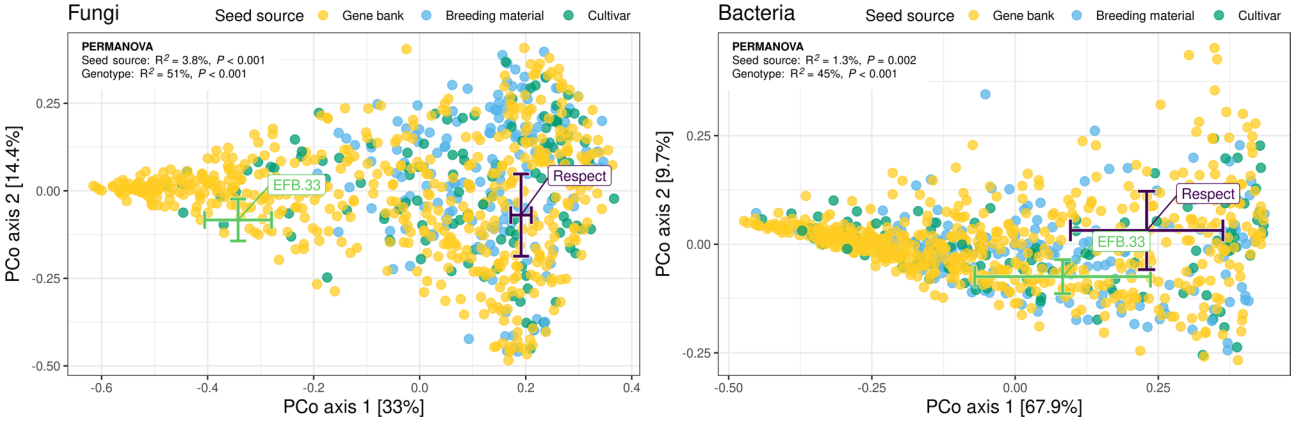

Fig. 2 Influence of plant genotype and seed source on root microbial beta diversity assessed by Principal Coordinates Analysis (PCoA) ordination of fungal and bacterial communities. Individual datapoints and means ± SE for two reference pea genotypes (EFB.33, Respect) are shown. PERMANOVA results with the explained variance (R^2) and the corresponding *P* value are included in both plots

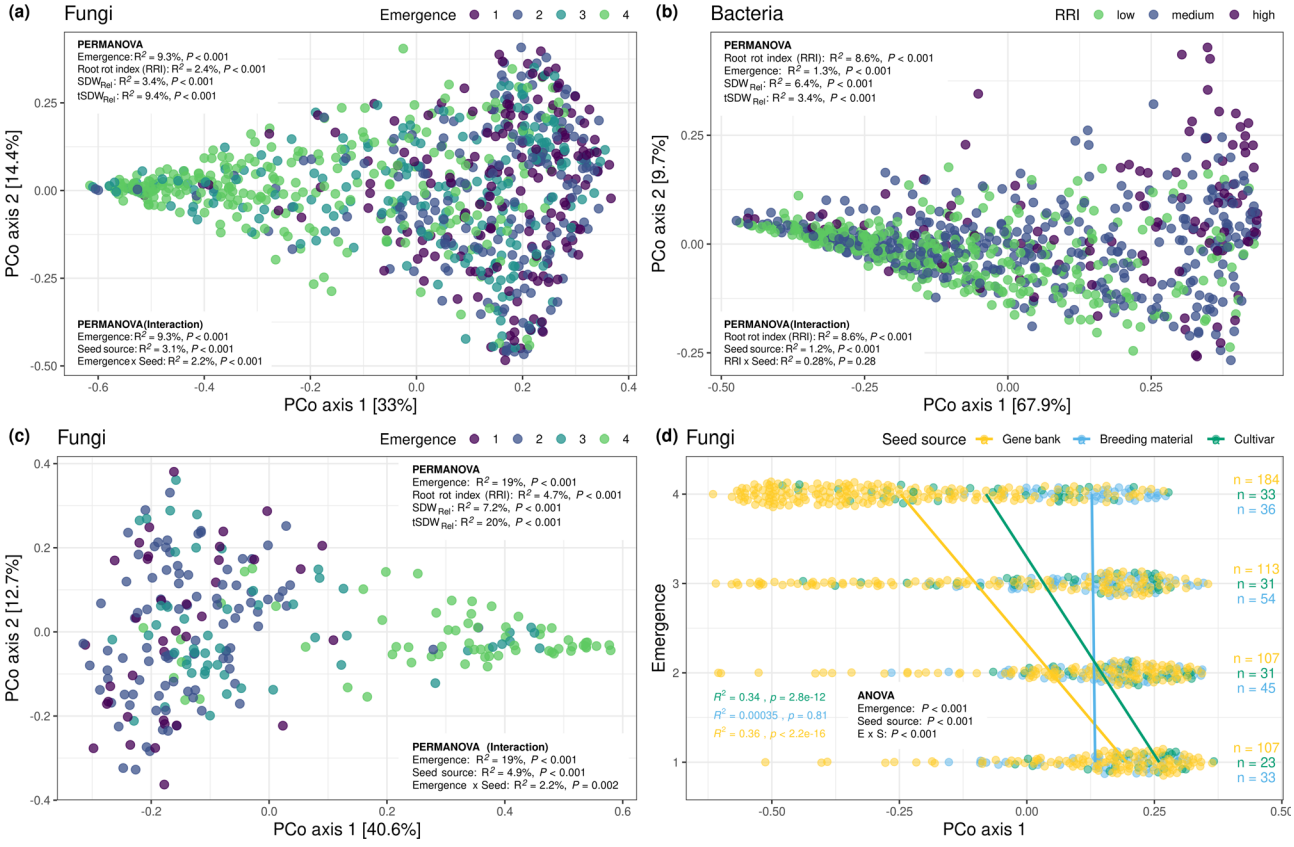

Fig. 3 Association of root fungal **(a**, **c**, **d)** and bacterial **(b)** beta diversity with root rot resistance assessed by Principal Coordinates Analysis (PCoA) ordination. **(a**, **b**, **c)** PERMANOVA results with the explained variances (R^2) and the corresponding *P* values for different root rot resistance-associated traits (top) and the interaction with seed source (bottom) are included. **(c)** PCoA and PERMANOVA results on means per genotype. **(d)** Correlation of emergence and fungal PCo axis 1 for each seed source. ANOVA table, as well as R^2 and *P* values of correlations for all seed sources are shown. The numbers of samples per emergence level and seed source are also indicated (n). SDW_{Rel}: Relative shoot dry weight per plant, $tSDW_{Rel}$: Relative total shoot dry weight per pot

material ($R^2 = 3.6\%$) and cultivars ($R^2 = 3.4\%$) but not for the breeding population.

Microbial diversity and resistance-associated OTUs are heritable

For alpha diversity indices (Shannon and OTU richness), the heritability (H^2; i.e. the proportion of variation explained by plant genotype) varied between 11% and 25%, with similar levels in both domains (Fig. 4a). By contrast, H^2 of beta diversity, summarized by PCo axis 1 and 2, was highly domain-specific (Fig. 4a). Whereas H^2 of bacterial community composition ($R^2 = 25.5\%$) was comparable to alpha diversity heritability, H^2 of the fungal PCo axis 1 was strikingly high ($R^2 = 70\%$). It is worth noting that these differences between bacterial and fungal heritabilities, or other traits, may also be a consequence of the different sequencing techniques used.

Fifty-eight OTUs showed an H^2 above 20% (Fig. 4b). Overall, fungal OTUs were more heritable (median $H^2 = 4.62\%$) than bacterial OTUs (median $H^2 = 2.3\%$; $P < 0.001$). Also, among the most heritable OTUs, there were significantly more fungi than bacteria; 48 out of the top 58 OTUs were fungi ($P < 0.001$). With a H^2 of 52%, fOTU1508 showed the highest H^2.

Fungal and bacterial OTUs were screened for their association with root rot resistance using the *ALDEx2* differential abundance pipeline. Fifty-one fungal and 34 bacterial OTUs were found to be associated with all resistance traits (Fig. 5a, b). These core differentially abundant OTUs either correlated with plant resistance (fungi: 35, bacteria: 13) or plant susceptibility (fungi: 17, bacteria: 21; Fig. 5c, d). Similarly to beta diversity, the highest number of resistance-associated OTUs were found for the traits emergence and $tSDW_{Rel}$ for fungi and RRI for

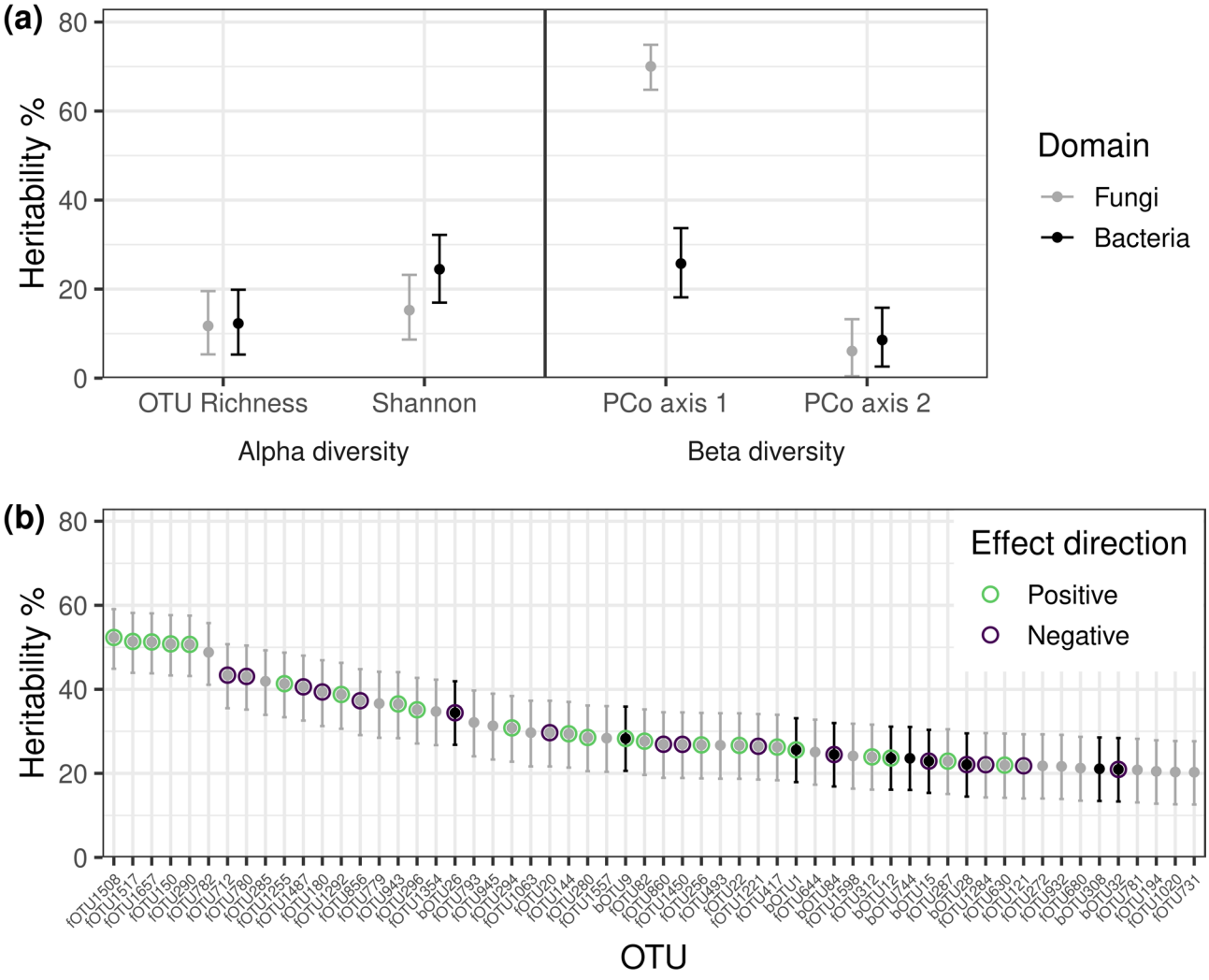

Fig. 4 Broad-sense heritability (H^2) of root microbial diversity and individual OTUs. **(a)** H^2 of alpha and beta diversity of fungi and bacteria. **(b)** H^2 of the 58 top heritable OTUs ($H^2 > 20\%$), including fungi (grey) and bacteria (black). OTUs positively (green) or negatively (purple) correlated with disease resistance are highlighted. **(a, b)** Bootstrap confidence intervals (95%) for H^2 are shown

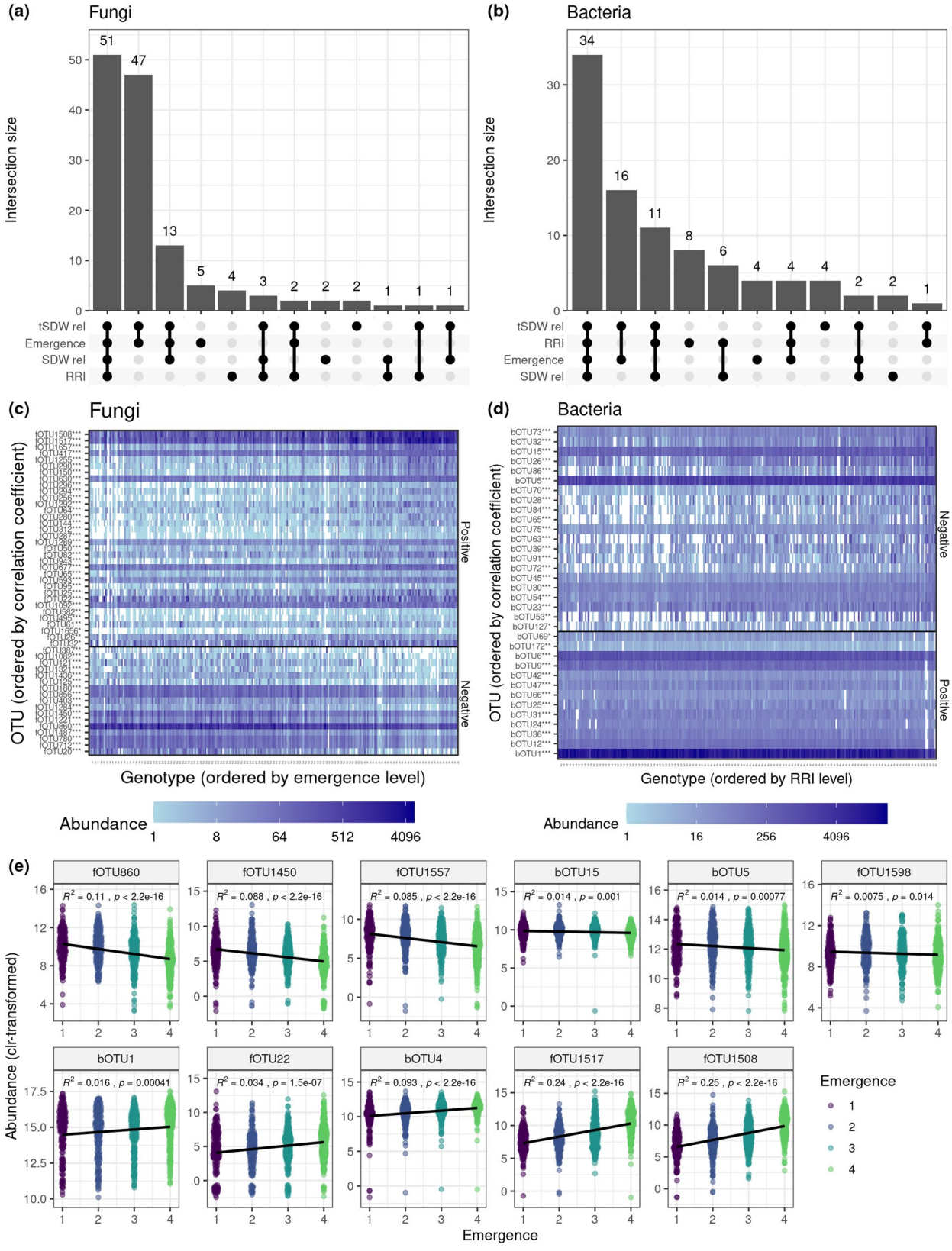

Fig. 5 (See legend on next page.)

(See figure on previous page.)

Fig. 5 Association of fungal **(a**, **c**, **e)** and bacterial **(b**, **d**, **e)** OTUs with root rot resistance traits. **(a**, **b)**. UpSet plots show the number of OTUs that are significantly correlated to root rot-associated traits and their intersection, where the first bar shows the OTUs that are significant for all traits. **(c**, **d)** Heat maps indicating the abundance OTUs significant for all traits, where the significance level is indicated with asterisks. The solid black line represents the transition from positive to negative correlation. Genotypes are ordered by increasing **(c)** emergence and **(d)** increasing RRI, and OTUs are ordered by their strength of correlation with the resistance trait. **(e)** Correlation of emergence and OTU abundance for OTUs with high relative abundance, connectedness in the microbial network, heritability and association with resistance. Explained variance (R^2) and *P* values of correlations are shown. SDW_{Rel}: Relative shoot dry weight per plant, $tSDW_{Rel}$: Relative total shoot dry weight per pot, RRI: Root rot index. Levels of significance: $P < 0.001$ ***, $P < 0.01$ **, $P < 0.05$ *

bacteria (Figs. 3 and 5a and b). Identical to the heritability analysis, fOTU1508 also exhibited the strongest association with root rot resistance ($R^2 = 24.5\%$).

Given the overlap of highly heritable OTUs and root rot-associated OTUs, we tested the hypothesis that H^2 is correlated with the magnitude of root rot resistance-association. Indeed, we found that an increase in root rot resistance-association was correlated with an increase in H^2 (Figure S9). This was observed to a similar extent for resistance- ($R^2 = 68\%$) and susceptibility-associated OTUs ($R^2 = 69\%$).

Network inference using the *SPIEC-EASI* pipeline revealed little overlap between nodes (OTUs) of the two domains (Figure S10). Further, most of the highly heritable and differentially abundant nodes are co-located within the network. Considering OTUs belonging to the top 10% (122 OTUs) of either betweenness or degree, we identified 172 hub OTUs.

To identify OTUs of potential high relevance, we selected hub OTUs that were (i) highly heritable (top 10%), (ii) highly linked to root rot resistance (top 10% of correlations of at least one resistance-associated trait), and (iii) abundant (relative abundance > 1%). Based on these requirements, we found 11 OTUs, seven fungi, and four bacteria (Table 1). Interestingly, all of these OTUs also showed a high prevalence, indicating that they were detected in most of the samples (ranging from 91.2 to 100%), while the majority of other OTUs were found to be less prevalent (Figure S11). Visualization of the association between OTU abundance and disease resistance of the selected OTUs further highlights that fungi are more associated (higher R^2) with emergence, whereas bacteria are more associated (higher R^2) with RRI (Fig. 5e and Figure S12).

Resistance- and susceptibility-associated OTUs are taxonomically diverse

To get a better understanding of the identified relevant resistance- and susceptibility-associated OTUs, we further investigated their taxonomic assignment. For fungi, the plant resistance-associated OTUs were *Dactylonectria* spp. (fOTU1508, fOTU1517; $r = 0.5$ and 0.49, $P < 0.001$) and *Olpidium* sp. (fOTU22; $r = 0.18$, $P < 0.001$; Table 1), the disease-associated OTUs were two *Fusarium* spp. (fOTU860, fOTU1450; r = -0.32 and −0.29, $P < 0.001$) and an OTU belonging to the Order Helotiales (fOTU1557; r = -0.29, $P < 0.001$). One putative *Fusarium* sp. (fOTU1598; r = -0.09, $P = 0.043$) was negatively correlated with emergence and RRI, thus associated with susceptibility (emergence) and resistance (RRI). For bacteria, the plant resistance-associated OTUs were a *Streptomyces* sp. (bOTU4; $r = 0.3$, $P < 0.001$) and a highly abundant, therefore likely nodule-inhabiting, *Rhizobium* sp. (bOTU1; $r = 0.14$, $P = 0.001$), and the disease-associated OTUs were another *Rhizobium* sp. (bOTU15; r = -0.12, $P = 0.006$) and a *Pseudomonas* sp. (bOTU5; r = -0.12, $P = 0.007$).

We further identified OTUs within our dataset belonging to taxa that are expected to relate to root rot and resistance to it [39]. Several of these additional candidate taxa were significantly associated with emergence and/or RRI (Table S1). As potential beneficial microbes, we searched for OTUs related to Arbuscular mycorrhizal fungi (AMF) and *Clonostachys rosea*. We found one OTU assigned to a *Funneliformis* sp. (fOTU1020, AMF), which was negatively correlated with RRI (r = -0.24, $P < 0.001$), and one putative *Clonostachys rosea* (fOTU60), which was weakly correlated with higher emergence ($r = 0.1$, $P = 0.018$; Table S1). As potential members of the root rot complex, we identified six *Fusarium* spp. (fOTU419, fOTU680, fOTU329, fOTU334, fOTU137, fOTU487) besides the ones reported above, one putative *Didymella pisi* (fOTU40; teleomorph of *Ascochyta pisi*), and four OTUs assigned to *Rhizoctonia* (fOTU831, fOTU578, fOTU140) or the synonymous genus *Ceratobasidium* (fOTU335, [80]). One *Fusarium* sp. (fOTU419; r = -0.14, $P < 0.001$), one *Rhizoctonia* sp. (fOTU831; r = -0.14, $P = 0.006$), and the putative *Ascochyta pisi* (fOTU40; r = -0.15, $P < 0.001$) were more abundant in low-emerging samples. Another *Fusarium* sp. (fOTU137, putative *Fusarium redolens*; r = -0.09, $P = 0.05$) was negatively correlated with RRI, and the remaining seven identified OTUs did not show any significant correlation.

Improved modeling of plant resistance through a combination of multiple OTUs and beta diversity

Comparing univariate models and stepwise regression models with OTU abundance and beta diversity revealed that 15 and 19 variables best explained (low AIC, high R^2) the disease resistance phenotypes emergence and RRI, respectively (Table S2, Table S3). For emergence, the explained variance of the univariate models with the most correlated OTU (fOTU1508, $R^2 = 22.8\%$) or the most correlated PCo axis (fungal PCo axis 1, $R^2 = 27.5\%$)

Table 1 Attributes of most root rot-associated, heritable, and interconnected OTUs. Taxonomy, relative abundance (RA), heritability, prevalence, network characteristics (degree and betweenness), and correlation (Spearman) with root rot resistance-associated traits of OTUs are listed. *P* values < 0.05 are highlighted in bold. Representative sequences can be found in Table S4

OTU id	Phylum	Family	Genus	Blast hit[A]	RA (%)[B]	Heritability (%)	Prevalence (%)	Degree	Betweenness	Emergence		RRI	
										r	*P*	*r*	*P*
fOTU860	Ascomycota	Nectriaceae	*Fusarium*	*Fusarium* sp.	10.8	26.9	100	21	5950	-0.322	< 0.001	0.118	0.006
fOTU1450	Ascomycota	Nectriaceae	unassigned	*Fusarium* sp.	1.33	26.8	96.7	21	3980	-0.291	< 0.001	0.168	< 0.001
fOTU1557	Ascomycota	unassigned	unassigned	Helotiales (Order)	2.64	28.3	99	19	6590	-0.288	< 0.001	-0.06	0.215
bOTU15	Proteobacteria	Rhizobiaceae	*Rhiobium**	*Rhizobium* sp.	1.47	23	99.9	67	17,900	-0.124	0.006	0.302	< 0.001
bOTU5	Proteobacteria	Pseudomonadaceae	*Pseudomonas*	*Pseudomonas* sp.	8.96	18.8	100	36	10,000	-0.123	0.007	0.244	< 0.001
fOTU1598	unassigned	unassigned	unassigned	*Fusarium* sp.	8.84	24.2	100	22	5600	-0.086	0.043	-0.118	0.006
bOTU1	Proteobacteria	Rhizobiaceae	*Rhizobium**	*Rhizobium* sp.	45.7	25.6	100	44	14,100	0.139	0.001	-0.35	< 0.001
fOTU22	unassigned	unassigned	unassigned	*Olpidium* sp.	1.46	26.5	91.1	20	4290	0.182	< 0.001	-0.35	< 0.001
bOTU4	Actinobacteriota	Streptomycetaceae	*Streptomyces*	*Streptomyces* sp.	3.46	13.7	99.3	34	7100	0.295	< 0.001	-0.052	0.471
fOTU1517	Ascomycota	Nectriaceae	*Dactylonectria*	*Dactylonectria* sp.	11.7	51.1	99.5	25	6660	0.488	< 0.001	-0.267	< 0.001
fOTU1508	Ascomycota	Nectriaceae	*Dactylonectria*	*Dactylonectria* sp.	8.31	52.3	99.5	36	8970	0.495	< 0.001	-0.322	< 0.001

[A]Top hit of a BLAST search against the NCBI database; [B]Within-Kingdom relative abundance was computed for each OTU

*,*Rhizobium*` refers to the genus `*Allorhizobium-Neorhizobium-Pararhizobium-Rhizobium*`

performed slightly worse compared to the stepwise regression OTU models without ($R^2 = 32.7\%$) and with beta diversity ($R^2 = 36.7\%$). For the RRI, the explained variance of the univariate models was markedly lower (bOTU1, $R^2 = 15\%$; bacterial PCo axis 1, $R^2 = 10.6\%$), while the stepwise regression model explained 33.9% (R^2) of the variance. Adding beta diversity measures did not increase model performance for RRI (Table S3).

Discussion

Plants are known to shape their associated microbiota in a genotype-specific manner [4, 81], which in turn affect plant growth and defense [1, 23]. To what extent microbiota attributes are associated with complex plant traits such as root rot resistance is largely unknown. The resistance of a given plant genotype against root rot was proposed to be influenced by individual known beneficial microbes [9, 39]. However, the extent to which the wider microbial community is associated with a genotype resistance is poorly understood. Here, we analyzed the root bacterial and fungal microbiota of a diverse set of pea genotypes grown under root rot stress and demonstrated that, in addition to individual key taxa, community-wide microbiota attributes are also associated with root rot resistance.

Our study reveals that associations, e.g. between root rot resistance and fungal and bacterial community composition, are driven by the individual pea genotypes. In line with our findings, common bean cultivars resistant to an individual fungal root pathogen (*Fusarium oxysporum)* were shown to harbor a distinct microbiota composition that is different from susceptible cultivars [82]. Our results expand these findings by investigating more than 250 genotypes in a field soil naturally infested with several pathogens, allowing us to show the range of microbial communities shaped by pea plants grown in the same soil. Notably, associations of fungal but not bacterial beta diversity were dependent on the seed source, with no correlation found for the Swiss breeding material (Fig. 3). This seed source dependency highlights the importance of screening plant microbiota interactions of large diversity panels. We demonstrate that the seed source effects are neglectable (alpha: 1-2.3%, beta: 1.3–3.8%) relative to the genotype effect (alpha diversity R^2: 16–25%, beta diversity R^2: 45–51%), even though within our panel the genotypic structure and phenotypic appearance of the modern European cultivars differ substantially from the gene bank accessions that mostly consists of landraces from around the world [38, 83]. Compared to the literature, the proportion of variance in beta diversity explained by the plant genotype was exceptionally high in our study [84]; in diversity panels of sorghum and maize, for example, the genotype effect on root microbiota composition was found to be 7.5%

and 9.8% [85, 86]. This could be due to stress conditions increasing the heritability of the root-associated microbiota [86]. Further, we report an increase in multivariate dispersion for gene bank accessions, indicative of a more variable set of microbiota communities. Thus, gene bank accessions could pose an interesting reservoir for microbiome-recruiting/manipulation alleles that are not present in breeding material or varieties, thereby supporting the breeding of microbiome-smart cultivars for sustainable agriculture [87]. However, given that the analyzed cultivars cover most of the microbial variation, they could also be used as a first source of desired alleles to speed up the introgression into elite cultivars due to the reduced number of unwanted alleles compared to gene bank accessions.

The abundance of individual OTUs can be determined by host genotype and have an impact on plant fitness [71]. In this study, we report multiple fungal and to some extent also bacterial OTUs that are associated with disease resistance or susceptibility (Fig. 5). The biggest portion of them is correlated with all the measured resistance phenotypes (root rot index (RRI), emergence, relative shoot dry weight per plant/pot), reflecting the magnitude of pathogen damage (RRI) as well as several plant performance measures. Given that root rot in peas is expected to be caused by fungal and oomycetous pathogens [29], the many bacterial OTUs found to be positively associated with RRI might have passively entered the roots through lesions or assisted as pathogen helper bacteria [88]. The higher bacterial alpha diversity in roots of diseased plants supports the hypothesis that bacteria can enter diseased roots more easily (Figure S6, Figure S7). In contrast, the resistance-associated bacterial and also fungal OTUs might directly or indirectly promote the plant health status or merely be spurious. Irrespective of a causal link, these key taxa show promise as resistance indicators in selection assays. It is striking that the OTUs that are correlated the most with resistance share several attributes: they generally have a high relative abundance, are highly interlinked with other OTUs (hub taxa), and are highly heritable (Table 1). The heritability of individual OTUs was markedly correlated with the degree of positive or negative disease association (Fig. S9), which could be explained either by root rot severity-dependent microbial root colonization [89] or by microbiota-mediated resistance to root pathogens [13, 26].

Investigating the taxonomy of the key OTUs (Table 1) revealed that the two most resistance-associated OTUs (fOTU1508, fOTU1517) belong to the genus of *Dactylonectria*. Various members of this genus have been associated with severe root disease in many annual and perennial plants like strawberries and grapevines [90–92]. Other studies found *Dactylonectria* spp. in asymptomatic roots of different plant species [3, 93], including the legume soybean, where members of this genus were shown to be enriched in the root endophytic community [94, 95]. To the best of our knowledge, this is the first report of *Dactylonectria* spp. being associated with disease resistance, highlighting this and other identified taxa as potential microbial markers to screen for root rot resistance in peas. The most susceptibility-associated OTUs were found to be *Fusarium* species. This underlines the well-investigated role of *Fusarium* spp. (e.g. *F. solani*, *F. oxysporum*) among the most prominent pathogens that cause pea root rot worldwide [29, 96]. Given that the selected primers do not amplify Oomycota, which include *Aphanomyces euteiches*, an important member of the pea root rot complex, we were not able to evaluate their contribution in our study. We, however, showed in a previous study [39] that *A. euteiches* was abundant in pea roots grown in infested soils but its association with root rot was minor across three diseased soils (including the one used in this study) compared to other known suspects and therefore not of high importance in the soil of this study. Several additional taxa associated with root rot were identified, suggesting that an even broader range of microbes may play a role in triggering root rot. Future experiments in different soils and under field conditions will show if the predictive power of the identified microbial markers can be translated to other environments. This will further evaluate the potential of microbiota-assisted disease resistance to improve agroecosystem sustainability.

Plant resistance is well-known to be heritable [97]. In our experimental system, the resistance to pea root pathogens was found to be highly heritable for emergence ($H^2 = 89\%$), followed by relative shoot dry weight ($H^2 = 51\%$) and root rot index ($H^2 = 43\%$, Wille et al., 2020). For the root microbiota, we report similar heritability levels of up to 52% for individual resistance-associated OTUs and 70% for the fungal community composition (beta diversity; Fig. 4). The abundance of single OTUs explained up to 22.8% (adjusted R^2) of the disease severity (Table S2). Combining the abundance of several OTUs with microbial community composition (PCoA axes) improved the prediction of root rot resistance to 36.7%. Incorporating information about the microbiota as decision support in the selection process of plant breeding could assist in promoting the beneficial root microbiota as a second line of defense against root pathogens. Genome-wide association studies and genomic prediction analysis will enable the identification of genetic loci associated with the potential recruitment of beneficial microbes and evaluate the joint use of microbial and plant markers [6].

Conclusion

This study provides evidence that plant genotype-specific root microbial communities and key taxa are associated with resistance to root rot in peas, highlighting their potential as microbial markers for plant breeding. This may pave the way for microbiome-assisted breeding to overcome the challenges currently faced in resistance breeding against root rot in legumes. Future research across diverse environments will be crucial to confirm the applicability of microbiome-assisted selection for resilient legume cultivation.

Supplementary Information

The online version contains supplementary material available at https://doi.org/10.1186/s40793-025-00755-w.

Supplementary Material 1

Acknowledgements
We thank the Genetic Diversity Centre (GDC) at ETH Zurich for their contribution to the processing of the raw sequencing reads.

Author contributions
MM, PH, and BS designed research. LW performed research. VG and MWH (QIIME2) analyzed data with input from MH, NB, MS, and PH. VG wrote the first draft of the manuscripts with input from PH, MH and MM. MM, MH, NB, MS, PH, KO contributed to the interpretation of the results and the writing of the manuscript. All authors approved the final version of the paper.

Funding
This research was supported by the Gebert Rüf Foundation (GRS-082/19), Root2Res (EU Horizon Europe no. 101060124 and Swiss State Secretariat for Education, Research and Innovation (SERI) no 23.00050), LIVESEED (EU Horizon 2020 no. 727230 and SERI no. 17.0009) and MICIU/AEI/https://doi.org/10.13039/501100011033 and FSE + under grant reference no RYC2022-037997-I. The opinions expressed and arguments employed herein do not necessarily reflect the official views of the EC and the Swiss government. Neither the European Commission, SERI nor any person acting on behalf of the Commission/SERI is responsible for the use which might be made of the information provided.

Data availability
The raw sequencing datasets are available in the European Nucleotide Archive (ENA, http://www.ebi.ac.uk/ena) at EMBL-EBI under the study accession PRJEB83630. R code and data to reproduce the statistical analysis and visualizations are available under https://github.com/ValentinGfeller/Gfeller_et_al_Microbiota_pea_panel.

Declarations

Ethics approval and consent to participate
Not applicable.

Consent for publication
Not applicable.

Competing interests
The authors declare no competing interests.

Received: 31 March 2025 / Accepted: 10 July 2025
Published online: 15 July 2025

References

1. Berendsen RL, Pieterse CMJ, Bakker PAHM. The rhizosphere Microbiome and plant health. Trends Plant Sci. 2012;17:478–86.
2. Trivedi P, Leach JE, Tringe SG, Sa T, Singh BK. Plant-microbiome interactions: from community assembly to plant health. Nat Rev Microbiol. 2020;18:607–21.
3. Durán P, Thiergart T, Garrido-Oter R, Agler M, Kemen E, Schulze-Lefert P, et al. Microbial interkingdom interactions in roots promote Arabidopsis survival. Cell. 2018;175:973–98314.
4. Bulgarelli D, Rott M, Schlaeppi K, Ver Loren Themaat E, Ahmadinejad N, Assenza F, et al. Revealing structure and assembly cues for Arabidopsis root-inhabiting bacterial microbiota. Nature. 2012;488:91–5.
5. Lundberg DS, Lebeis SL, Paredes SH, Yourstone S, Gehring J, Malfatti S, et al. Defining the core Arabidopsis thaliana root Microbiome. Nature. 2012;488:86–90.
6. Escudero-Martinez C, Bulgarelli D. Engineering the crop microbiota through host genetics. Annu Rev Phytopathol. 2023;61:257–77.
7. Hu L, Robert CAM, Cadot S, Zhang X, Ye M, Li B, et al. Root exudate metabolites drive plant-soil feedbacks on growth and defense by shaping the rhizosphere microbiota. Nat Commun. 2018;9:2738.
8. Gfeller V, Thoenen L, Erb M. Root-exuded benzoxazinoids can alleviate negative plant–soil feedbacks. New Phytol. 2024;241:2575–88.
9. Wille L, Messmer MM, Studer B, Hohmann P. Insights to plant–microbe interactions provide opportunities to improve resistance breeding against root diseases in grain legumes. Plant Cell Environ. 2019;42:20–40.
10. Savary S, Willocquet L, Pethybridge SJ, Esker P, McRoberts N, Nelson A. The global burden of pathogens and pests on major food crops. Nat Ecol Evol. 2019;3:430–9.
11. Singh BK, Delgado-Baquerizo M, Egidi E, Guirado E, Leach JE, Liu H, et al. Climate change impacts on plant pathogens, food security and paths forward. Nat Rev Microbiol. 2023;21:640–56.
12. Busby PE, Soman C, Wagner MR, Friesen ML, Kremer J, Bennett A, et al. Research priorities for Harnessing plant microbiomes in sustainable agriculture. PLoS Biol. 2017;15:e2001793.
13. Vannier N, Agler M, Hacquard S. Microbiota-mediated disease resistance in plants. PLoS Pathog. 2019;15:e1007740.
14. Entila F, Han X, Mine A, Schulze-Lefert P, Tsuda K. Commensal lifestyle regulated by a negative feedback loop between Arabidopsis ROS and the bacterial T2SS. Nat Commun. 2024;15:456.
15. Ma K-W, Niu Y, Jia Y, Ordon J, Copeland C, Emonet A, et al. Coordination of microbe–host homeostasis by crosstalk with plant innate immunity. Nat Plants. 2021;7:814–25.
16. Pereira LB, Thomazella DPT, Teixeira PJPL. Plant-microbiome crosstalk and disease development. Curr Opin Plant Biol. 2023;72:102351.
17. Berendsen RL, Vismans G, Yu K, Song Y, de Jonge R, Burgman WP, et al. Disease-induced assemblage of a plant-beneficial bacterial consortium. ISME J. 2018;12:1496–507.
18. Liu S, Tao C, Zhang L, Wang Z, Xiong W, Xiang D, et al. Plant pathogen resistance is mediated by recruitment of specific rhizosphere fungi. ISME J. 2023;17:931–42.
19. Caballero-Flores G, Pickard JM, Núñez G. Microbiota-mediated colonization resistance: mechanisms and regulation. Nat Rev Microbiol. 2023;21:347–60.
20. Chen Y, Wang J, Yang N, Wen Z, Sun X, Chai Y, et al. Wheat Microbiome bacteria can reduce virulence of a plant pathogenic fungus by altering histone acetylation. Nat Commun. 2018;9:3429.
21. Gu S, Wei Z, Shao Z, Friman V-P, Cao K, Yang T, et al. Competition for iron drives phytopathogen control by natural rhizosphere microbiomes. Nat Microbiol. 2020;5:1002–10.
22. Matsumoto H, Fan X, Wang Y, Kusstatscher P, Duan J, Wu S, et al. Bacterial seed endophyte shapes disease resistance in rice. Nat Plants. 2021;7:60–72.
23. Pieterse CMJ, Zamioudis C, Berendsen RL, Weller DM, van Wees SCM, Bakker PAHM. Induced systemic resistance by beneficial microbes. Annu Rev Phytopathol. 2014;52:347–75.
24. Shoresh M, Harman GE, Mastouri F. Induced Systemic Resistance and Plant Responses to Fungal Biocontrol Agents. Annual Review of Phytopathology. 2010;48 Volume 48, 2010:21–43.
25. Carrión VJ, Perez-Jaramillo J, Cordovez V, Tracanna V, Hollander M, Ruiz-Buck D, et al. Pathogen-induced activation of disease-suppressive functions in the endophytic root Microbiome. Science. 2019;366:606–12.
26. Jian Y, Gong D, Wang Z, Liu L, He J, Han X, et al. How plants manage pathogen infection. EMBO Rep. 2024;25:31–44.

27. Stagnari F, Maggio A, Galieni A, Pisante M. Multiple benefits of legumes for agriculture sustainability: an overview. Chem Biol Technol Agric. 2017;4:2.
28. Tulbek MC, Lam RSH, Wang Y, C., Asavajaru P, Lam A. Chapter 9 - Pea: A sustainable vegetable protein crop. In: Nadathur SR, Wanasundara JPD, Scanlin L, editors. Sustainable protein sources. San Diego: Academic; 2017. pp. 145–64.
29. Harveson RM, Pasche JS, Porter L, Chen W, Burrows M, editors. Compendium of pea diseases and pests. Third edition. St. Paul, Minnesota: The American Phytopathological Society; 2021.
30. Sharma A, Rani M, Lata H, Thakur A, Sharma P, Kumar P, et al. Global dimension of root rot complex in garden pea: current status and breeding prospective. Crop Prot. 2022;158:106004.
31. Alcala AVC, Paulitz TC, Schroeder KL, Porter LD, Derie ML, du Toit LJ. Pythium species associated with Damping-off of pea in certified organic fields in the Columbia basin of central Washington. Plant Dis. 2016;100:916–25.
32. Esmaeili Taheri A, Chatterton S, Foroud NA, Gossen BD, McLaren DL. Identification and community dynamics of fungi associated with root, crown, and foot rot of field pea in Western Canada. Eur J Plant Pathol. 2017;147:489–500.
33. Gaulin E, Jacquet C, Bottin A, Dumas B. Root rot disease of legumes caused by Aphanomyces euteiches. Mol Plant Pathol. 2007;8:539–48.
34. Pflughöft O, Merker C, von Tiedemann A, Schäfer BC. Zur verbreitung und bedeutung von Pilzkrankheiten in Körnerfuttererbsen (Pisum sativum L.) in Deutschland. Gesunde Pflanzen. 2012;64:39–48.
35. Baćanović-Šišić J, Šišić A, Schmidt JH, Finckh MR. Identification and characterization of pathogens associated with root rot of winter peas grown under organic management in Germany. Eur J Plant Pathol. 2018;151:745–55.
36. Chatterton S, Harding MW, Bowness R, Mclaren DL, Banniza S, Gossen BD. Importance and causal agents of root rot on field pea and lentil on the Canadian prairies, 2014–2017. Can J Plant Pathol. 2019;41:98–114.
37. Rubiales D, Fondevilla S, Chen W, Gentzbittel L, Higgins TJV, Castillejo MA, et al. Achievements and challenges in legume breeding for pest and disease resistance. CRC Crit Rev Plant Sci. 2015;34:195–236.
38. Wille L, Messmer MM, Bodenhausen N, Studer B, Hohmann P. Heritable variation in pea for resistance against a root rot complex and its characterization by amplicon sequencing. Front Plant Sci. 2020;11.
39. Wille L, Kurmann M, Messmer MM, Studer B, Hohmann P. Untangling the pea root rot complex reveals microbial markers for plant health. Front Plant Sci. 2021;12:737820.
40. Chatterton S, Yang HE, Ortega Polo R, McAllister TA, Safarieskandari S, Lupwayi N. Bacterial and fungal communities, but not physicochemical properties, of soil differ according to root rot status of pea. Pedobiologia. 2021;84:150705.
41. Hossain Z, Hubbard M, Gan Y, Bainard LD. Root rot alters the root-associated Microbiome of field pea in commercial crop production systems. Plant Soil. 2021;460:593–607.
42. Gardes M, Bruns TD. ITS primers with enhanced specificity for basidiomycetes–application to the identification of mycorrhizae and rusts. Mol Ecol. 1993;2:113–8.
43. White TJ, Bruns T, Lee S, Taylor J. Amplification and direct sequencing of fungal ribosomal RNA genes for phylogenetics. PCR Protocols: Guide Methods Appl. 1990;18:315–22.
44. Chakravorty S, Helb D, Burday M, Connell N, Alland D. A detailed analysis of 16S ribosomal RNA gene segments for the diagnosis of pathogenic bacteria. J Microbiol Methods. 2007;69:330–9.
45. Chelius MK, Triplett EW. The diversity of Archaea and Bacteria in association with the roots of Zea mays L. Microb Ecol. 2001;41:252–63.
46. Edgar RC. UPARSE: highly accurate OTU sequences from microbial amplicon reads. Nat Methods. 2013;10:996–8.
47. Edgar RC. UNOISE2: improved error-correction for illumina 16S and ITS amplicon sequencing. BioRxive. 2016. https://doi.org/10.1101/081257.
48. Callahan BJ, McMurdie PJ, Rosen MJ, Han AW, Johnson AJA, Holmes SP. DADA2: High-resolution sample inference from illumina amplicon data. Nat Methods. 2016;13:581–3.
49. Estensmo ELF, Maurice S, Morgado L, Martin-Sanchez PM, Skrede I, Kauserud H. The influence of intraspecific sequence variation during DNA metabarcoding: A case study of eleven fungal species. Mol Ecol Resour. 2021;21:1141–8.
50. Pan P, Gu Y, Sun D-L, Wu QL, Zhou N-Y. Microbial diversity biased Estimation caused by intragenomic heterogeneity and interspecific conservation of 16S rRNA genes. Appl Environ Microbiol. 2023;89:e02108–22.
51. Stadler M, Lambert C, Wibberg D, Kalinowski J, Cox RJ, Kolařík M, et al. Intragenomic polymorphisms in the ITS region of high-quality genomes of the hypoxylaceae (Xylariales, Ascomycota). Mycol Progress. 2020;19:235–45.
52. Schloss PD. Amplicon sequence variants artificially split bacterial genomes into separate clusters. mSphere. 2021;6. https://doi.org/10.1128/msphere.00191-21.
53. Edgar RC. SINTAX: a simple non-Bayesian taxonomy classifier for 16S and ITS sequences. BioRxive.2016. https://doi.org/10.1101/074161
54. Nilsson RH, Larsson K-H, Taylor AFS, Bengtsson-Palme J, Jeppesen TS, Schigel D, et al. The UNITE database for molecular identification of fungi: handling dark taxa and parallel taxonomic classifications. Nucleic Acids Res. 2019;47:259–64.
55. Bolyen E, Rideout JR, Dillon MR, Bokulich NA, Abnet CC, Al-Ghalith GA, et al. Reproducible, interactive, scalable and extensible Microbiome data science using QIIME 2. Nat Biotechnol. 2019;37:852–7.
56. Mittelstrass J, Sperone FG, Horton MW. Using transects to disentangle the environmental drivers of plant-microbiome assembly. Plant Cell Environ. 2021;44:3515–25.
57. Rognes T, Flouri T, Nichols B, Quince C, Mahé F. VSEARCH: a versatile open source tool for metagenomics. PeerJ. 2016;4:e2584.
58. Quast C, Pruesse E, Yilmaz P, Gerken J, Schweer T, Yarza P, et al. The SILVA ribosomal RNA gene database project: improved data processing and web-based tools. Nucleic Acids Res. 2013;41Database issue:590–6.
59. Wang Q, Garrity GM, Tiedje JM, Cole JR. Naïve bayesian classifier for rapid assignment of rRNA sequences into the new bacterial taxonomy. Appl Environ Microbiol. 2007;73:5261–7.
60. R Core Team. R: A Language and Environment for Statistical Computing. 2023.
61. Wickham H, Averick M, Bryan J, Chang W, McGowan L, François R, et al. Welcome to the tidyverse. JOSS. 2019;4:1686.
62. Wilke CO. cowplot: Streamlined Plot Theme and Plot Annotations for ggplot2. 2020.
63. Clarke E, Sherrill-Mix S, Dawson C. ggbeeswarm: Categorical Scatter (Violin Point) Plots. 2023.
64. McMurdie PJ, Holmes S. Phyloseq: an R package for reproducible interactive analysis and graphics of Microbiome census data. PLoS ONE. 2013;8:61217.
65. Oksanen J, Blanchet FG, Friendly M, Kindt R, Legendre P, McGlinn D et al. vegan: Community Ecology Package. 2020.
66. Lenth RV. emmeans: Estimated Marginal Means, aka Least-Squares Means. 2022.
67. Hothorn T, Bretz F, Westfall P. Simultaneous inference in general parametric models. Biom J. 2008;50:346–63.
68. Anderson MJ, Walsh DCI. PERMANOVA, ANOSIM, and the mantel test in the face of heterogeneous dispersions: what null hypothesis are you testing? Ecol Monogr. 2013;83:557–74.
69. Fernandes AD, Reid JN, Macklaim JM, McMurrough TA, Edgell DR, Gloor GB. Unifying the analysis of high-throughput sequencing datasets: characterizing RNA-seq, 16S rRNA gene sequencing and selective growth experiments by compositional data analysis. Microbiome. 2014;2:15.
70. Bruijning M, Ayroles JF, Henry LP, Koskella B, Meyer KM, Metcalf CJE. Relative abundance data can misrepresent heritability of the Microbiome. Microbiome. 2023;11:222.
71. Brachi B, Filiault D, Whitehurst H, Darme P, Le Gars P, Le Mentec M et al. Plant genetic effects on microbial hubs impact host fitness in repeated field trials. Proceedings of the National Academy of Sciences. 2022;119.
72. Bates D, Mächler M, Bolker B, Walker S. Fitting linear Mixed-Effects models using lme4. J Stat Soft. 2015;67.
73. Nearing JT, Douglas GM, Hayes MG, MacDonald J, Desai DK, Allward N, et al. Microbiome differential abundance methods produce different results across 38 datasets. Nat Commun. 2022;13:342.
74. Benjamini Y, Hochberg Y. Controlling the false discovery rate: A practical and powerful approach to multiple testing. J Roy Stat Soc: Ser B (Methodol). 1995;57:289–300.
75. Ahlmann-Eltze C. ggupset: Combination Matrix Axis for ggplot2 to Create UpSet Plots. 2025.
76. Kurtz ZD, Müller CL, Miraldi ER, Littman DR, Blaser MJ, Bonneau RA. Sparse and compositionally robust inference of microbial ecological networks. PLoS Comput Biol. 2015;11:e1004226.
77. Tipton L, Müller CL, Kurtz ZD, Huang L, Kleerup E, Morris A, et al. Fungi stabilize connectivity in the lung and skin microbial ecosystems. Microbiome. 2018;6:12.
78. Csárdi G, Nepusz T, Müller K, Horvát S, Traag V, Zanini F et al. igraph for R: R interface of the igraph library for graph theory and network analysis. 2024.
79. Ripley B, Venables B, ca Bates DM. 1998) KH (partial port, ca 1998) AG (partial port, polr) DF (support functions for. MASS: Support Functions and Datasets for Venables and Ripley's MASS. 2024.

80. Oberwinkler F, Riess K, Bauer R, Kirschner R, Garnica S. Taxonomic re-evaluation of the Ceratobasidium-Rhizoctonia complex and rhizoctonia butinii, a new species attacking Spruce. Mycol Progress. 2013;12:763–76.
81. Horton MW, Bodenhausen N, Beilsmith K, Meng D, Muegge BD, Subramanian S, et al. Genome-wide association study of Arabidopsis thaliana leaf microbial community. Nat Commun. 2014;5:5320.
82. Mendes LW, Raaijmakers JM, De Hollander M, Mendes R, Tsai SM. Influence of resistance breeding in common bean on rhizosphere Microbiome composition and function. ISME J. 2018;12:212–24.
83. Ariza-Suarez D, Wille L, Hohmann P, Gfeller V, Schneider M, Horton M et al. Association genetics and genomic prediction for resistance to root rot in a diverse collection of Pisum sativum L. Authorea. 2024. https://doi.org/10.22541/au.172517490.04797375/v1
84. Wagner MR. Prioritizing host phenotype to understand Microbiome heritability in plants. New Phytol. 2021;232:502–9.
85. Deng S, Caddell DF, Xu G, Dahlen L, Washington L, Yang J, et al. Genome wide association study reveals plant loci controlling heritability of the rhizosphere Microbiome. ISME J. 2021;15:3181–94.
86. He X, Wang D, Jiang Y, Li M, Delgado-Baquerizo M, McLaughlin C, et al. Heritable Microbiome variation is correlated with source environment in locally adapted maize varieties. Nat Plants. 2024;10:598–617.
87. Nerva L, Sandrini M, Moffa L, Velasco R, Balestrini R, Chitarra W. Breeding toward improved ecological plant–microbiome interactions. Trends Plant Sci. 2022;27:1134–43.
88. Li M, Pommier T, Yin Y, Wang J, Gu S, Jousset A, et al. Indirect reduction of *Ralstonia solanacearum* via pathogen helper Inhibition. ISME J. 2022;16:868–75.
89. Larousse M, Rancurel C, Syska C, Palero F, Etienne C, Industri B, et al. Tomato root microbiota and Phytophthora parasitica-associated disease. Microbiome. 2017;5:56.
90. CARLUCCI A, LOPS F, HALLEEN MOSTERTL, RAIMONDO F. ML. Occurrence fungi causing black foot on young grapevines and nursery rootstock plants in Italy. Phytopathologia Mediterranea. 2017;56.
91. Manici LM, Kelderer M, Caputo F, Saccà ML, Nicoletti F, Topp AR, et al. Involvement of dactylonectria and ilyonectria spp. In tree decline affecting multigeneration Apple orchards. Plant Soil. 2018;425:217–30.
92. Weber RWS, Entrop A-P. Dactylonectria torresensis as the main component of the black root rot complex of strawberries and raspberries in Northern Germany. Erwerbs-Obstbau. 2017;59:157–69.
93. Berlanas C, Ojeda S, López-Manzanares B, Andrés-Sodupe M, Bujanda R, Del Pilar Martínez-Diz M, et al. Occurrence and diversity of Black-Foot disease Fungi in symptomless grapevine nursery stock in Spain. Plant Dis. 2020;104:94–104.
94. Moroenyane I, Tremblay J, Yergeau É. Temporal and Spatial interactions modulate the soybean Microbiome. FEMS Microbiol Ecol. 2021;97:fiaa2062.
95. Strom N, Hu W, Haarith D, Chen S, Bushley K. Corn and soybean host root endophytic Fungi with toxicity toward the soybean cyst nematode. Phytopathology®. 2020;110:603–14.
96. Bani M, Pérez-De-Luque A, Rubiales D, Rispail N. Physical and chemical barriers in root tissues contribute to quantitative resistance to fusarium oxysporum f. Sp. pisi in pea. Front Plant Sci. 2018;9:199.
97. Hammond-Kosack KE, Jones JD. Resistance gene-dependent plant defense responses. Plant Cell. 1996;8:1773–91.

Publisher's note